DOI: https://doi.org/10.37434/tpwj2024.07.01

MANUFACTURING A CONSOLIDATED COPPER-STAINLESS STEEL BIMETALLIC PRODUCT USING xBeam 3D METAL PRINTING

D. Kovalchuk[1], L. Tretiakov[1], P.R. Carriere[2], Nanda Gopal Matavalam[2]

[1]JSC NVO Chervona Hvilya
28 Dubrovytska Str., 04200, Kyiv, Ukraine
[2]RadiaBeam Technologies, LLC
1717 Stewart Str., Santa Monica, CA 90404, USA

ABSTRACT

The creation of strong and tight copper and stainless steel joints in mechanical structures and components is an actual challenge in modern engineering. Thanks to unique combination of different properties such joints have many important applications like components of linear particle accelerators, ultra-high vacuum systems (up to 10^{-8} torr), heat exchangers, even of the international fusion experimental reactor. At the same time, ensuring a reliable joint of immiscible materials such as copper and stainless steel is a technologically challenging problem due to significantly different physical, mechanical and metallurgical properties, including melting points, thermal expansion coefficients, thermal conductivity, etc. Traditional approaches to the production of such joints, based on certain welding methods, impose many technical and geometric limitations due to the need for special preparation of the contact surfaces of the parts to be joined or the uncontrolled formation of new phases when mixing melts of different metals. As for brazing methods, they do not always provide reliable vacuum-tight joints for relatively thick parts and do not guarantee sufficient joint strength. Therefore, it is important to find more technologically flexible ways to solve such problems. This article discusses a new approach to joining copper and stainless steel using the xBeam 3D Metal Printing technology. This novel directed energy deposition (DED) technology uses a profile electron beam and coaxial feeding of copper wire to deposit it upon a precision machined stainless steel substrate. The results of the exploration study of joints made using this method are presented, including the study of vacuum tightness of the joint, density of the deposited material, metallurgy of the interface, electrical conductivity, oxygen content, hardness in different zones, etc. Specialized preheating strategies minimized the thermal deformation of the machined substrate, a key consideration for adding multimaterial functionality to monolith components.

KEYWORDS: copper, stainless steel, joining, bimetals, additive manufacturing, metal 3D printing, electron beam, DED-wire

INTRODUCTION

Complex consolidated assemblies of different materials are used in various industries due to the ability to optimally combine the best mechanical, thermal and chemical properties in one product, which cannot be achieved by manufacturing from a single material. In particular, the bimetallic combination of copper and stainless steel is of great interest, as it creates a unique combination of excellent properties. Stainless steel combines high strength, satisfactory ductility, and low thermal conductivity, while copper has high thermal and electrical conductivity, high ductility, as well. Both materials have good corrosion resistance in various environments. Due to this combination of properties, consolidated copper and stainless steel bimetallic products are used in critical components of nuclear reactors, linear accelerators, ultrahigh-vacuum equipment, thin film deposition systems, heat exchangers, experimental physics environments, etc.

However, obtaining a reliable joint of copper and stainless steels is a technologically challenging task due to significantly different thermophysical, mechanical and metallurgical properties, such as melting point and heat of fusion, thermal expansion coefficients, thermal conductivity, viscosity, surface tension coefficients, etc. It is also worth considering that stainless steel is an alloy of Fe–Cr–Ni (along with a number of impurities such as C, Si, Mn, S, P and Cu), while copper is a pure metal element. This requires attention to physical and chemical aspects of the interaction between these materials when joining them.

Various methods of joining copper and stainless steel, both in the solid state and through melt contact, are known, including diffusion joining [1], various welding and brazing processes [2–5], and 3D printing processes using lasers or traditional thermionic electron beam guns as heating sources and consumables in the form of powder or wire [6–7]. However, each process has certain limitations and issues, so the task of developing new methods for creating bimetallic combinations of copper and stainless steel remains relevant.

STATEMENT OF WORK

In this paper, the authors demonstrate a methodology for producing a consolidated product in the form

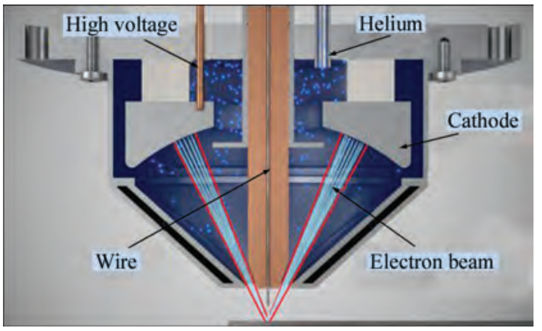

Figure 1. Formation of an electron beam in the form of a hollow inverted cone in xBeam 3D metal printing technology

of a thick-walled, high-purity copper cylinder tightly attached to a preprecision machined stainless steel flange (Conflat™) using xBeam metal 3D printing technology.

Conflat flanges are routinely in vacuum systems as part of demountable assembly method. Conflats are particular useful for achieving ultra-high vacuum, as they copper gasket enables higher bakeout temperatures than conventional polymeric gaskets while also providing a helium-impermeable barrier. The seal is formed via a knife edge machined into the stainless steel which plastically deforms, or bites, into the softer copper gasket. Unlike polymer o-rings sealing methods, the form and finish of a conflat knife edge must be much more precise. Flatness of the knife edge is critically important, as the shallow (0.5 mm) knife edge must uniformly engage with the copper gasket. The flatness and dimensions of the knife edge are therefore critical, as they must ensure perfectly uniform contact with the copper sealing gasket.

The xBeam metal 3D printing technology was chosen for this study due to the excellent control of thermal processes in and around the melt pool during the layer-by-layer formation of the deposited product, which allowed us to expect, firstly, the formation of a consolidated joint between two materials with different physical properties, and secondly, minimization of residual distortions of the machined substrate, since their processing after depositing the copper cylinder is not allowed.

The xBeam metal 3D printing technology uses a hollow conical profile electron beam as a heating source, which is directly generated by a gas discharge electron gun, and a wire is used as a feedstock for deposition, which is fed coaxially with the mentioned profile electron beam directly into the center of the deposition zone [8] (Figure 1). This configuration allows the same electron beam to create a melt pool on the substrate and simultaneously melt the feedstock wire above the melt pool, reducing the thermal impact on the substrate material and controlling the melt pool parameters well [9] (Figure 2) — this is especially important to avoid excessive mixing of the two different materials and the corresponding impact of the difference in their physical and chemical properties.

The moderate energy density of the low-voltage (<20 kV) electron beam and the dispersed edges of the beam focus significantly reduce the temperature gradients in the substrate material and the previously printed layers of the added material. This gradual temperature gradient reduces the thermally induced stress gradients, thus minimizing cracking, residual stresses and deformation [10].

EXPERIMENT

The experiment was conducted on the xBeamLab laboratory 3D printing system.

Standard commercial conflates DN35-DN40 with an outer diameter of 69.85 mm (2.75″ OD) made of 304L stainless steel were used for the experiments (Figure 3). The metal-to-metal sealing edge of this conflate is made on an inner diameter of 41.91 mm (1.650″). These conflates were used as substrates for

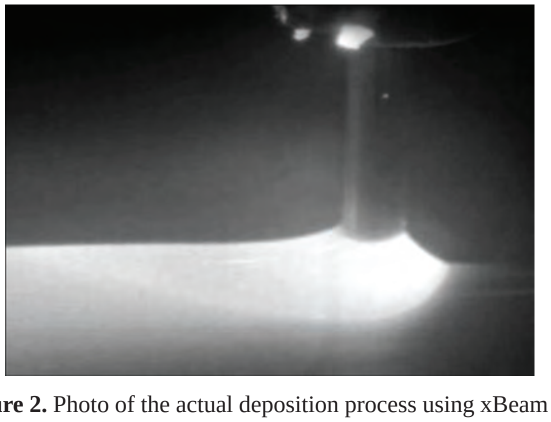

Figure 2. Photo of the actual deposition process using xBeam 3D metal printing technology

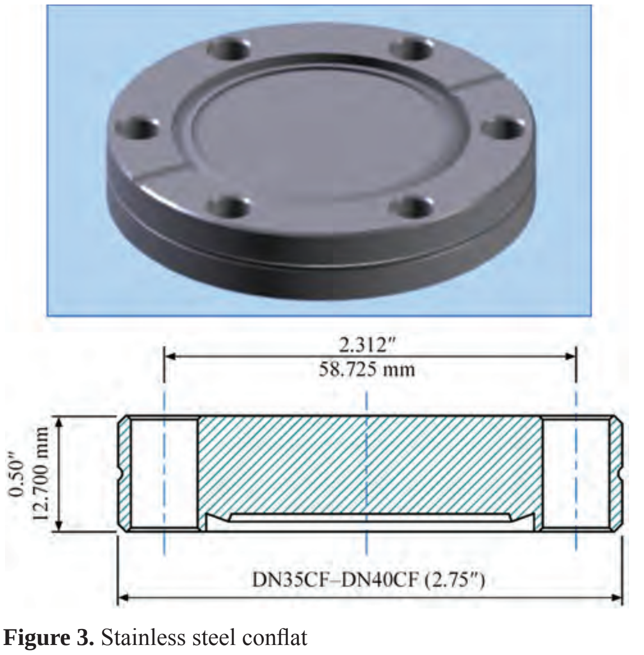

Figure 3. Stainless steel conflat

the deposition of pure copper wire with subsequent layer-by-layer build-up of copper cylinders using xBeam 3D metal printing technology. The final dimensions of the copper cylinders after finishing were set (Figure 4), accordingly, technologists determined the parameters of the model for 3D printing, taking into account allowances for processing. At the same time, any processing of conflates after the production of the consolidated product was not allowed.

A 2 mm diameter wire of pure copper grade M1 (Cu > 99.9 %, oxygen content no more than 20 ppm) was used as a feedstock for deposition. Since the oxygen content of copper is critical for high-vacuum applications, pure helium (99.995 %) was used as the working gas of the gas-discharge electron beam gun to minimize the absorption of oxygen from the residual atmosphere of the operating chamber.

Heating processes, i.e. turning on the electron beam gun, started at a vacuum of $5 \cdot 10^{-2}$ mbar. Then the residual pressure in the operating chamber was increased due to the supply of operating gas to the EB gun, and the technological 3D printing process was carried out at a partial pressure of helium of $3–5 \cdot 10^{-1}$ mbar.

The Conflat substrate was placed in cylindrical sockets made in a thick copper plate. Such a decision made it possible to carry out preliminary indirect heating of the conflates before deposition by means of heat conduction from a copper plate, which was slowly heated by an electron beam for a certain time. The gradual heating of the substrate stabilized the processing temperature and reduced the thermal gradients. Specifically, the heat deposited into the part from the molten copper is balanced against radiative heat loss into the surrounding processing chamber as well as conduction loss into the deposition fixture. By stabilizing these temperature profiles with a large, preheated thermal mass, the internal stresses in the body during printing is reduced.

After preliminary heating of the substrates (conflates), copper wire was deposited on them. On each layer, the wire was deposited with two coaxial rings of different diameters to form the required thickness of the cylinder wall, taking into account the allowance for its finishing mechanical processing.

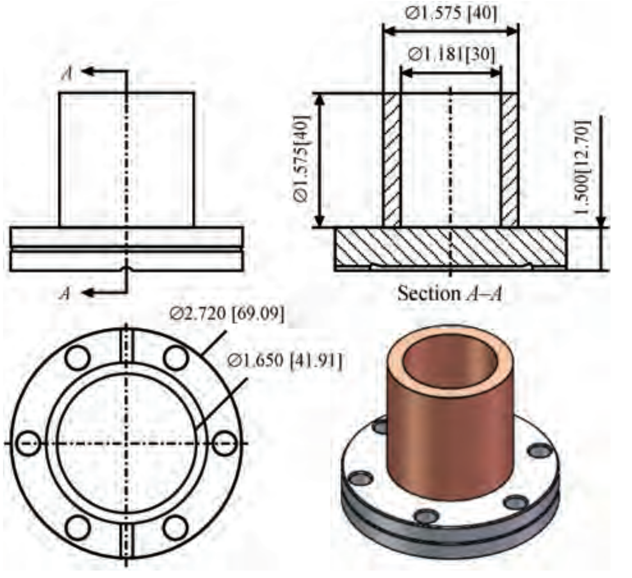

Figure 4. Dimensions of the final consolidated product

The thickness of the layer when forming the copper cylinder was 1.4 mm with a wire feed rate of 14 mm/s. The power of the electron beam was from 5 to 5.5 kW at an accelerating voltage of 18 kV while the deposition travel speed was set to 10mm/sec. This made it possible to deposit 2 mm copper wire with a net productivity of about 1.4 kg/h. To prevent excessive heat accumulation in the 3D printed material, pauses were used before starting to print the next layer. Considering all technological factors, the complete printing time of one consolidated product was about 40 minutes.

INVESTIGATION OF SAMPLES AND DISCUSSION

As a result, four samples were produced, one of which (Figure 5) was used to conduct a number of exploratory studies, including metallographic analysis of the consolidation zone of the two materials, determina-

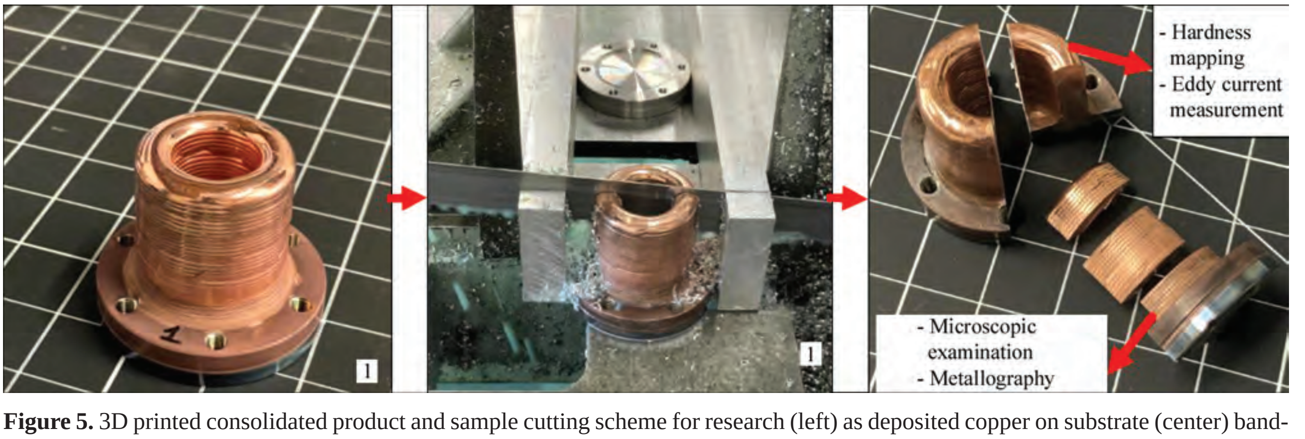

Figure 5. 3D printed consolidated product and sample cutting scheme for research (left) as deposited copper on substrate (center) band-saw cutting of sample for analysis (right) sectioning of sample

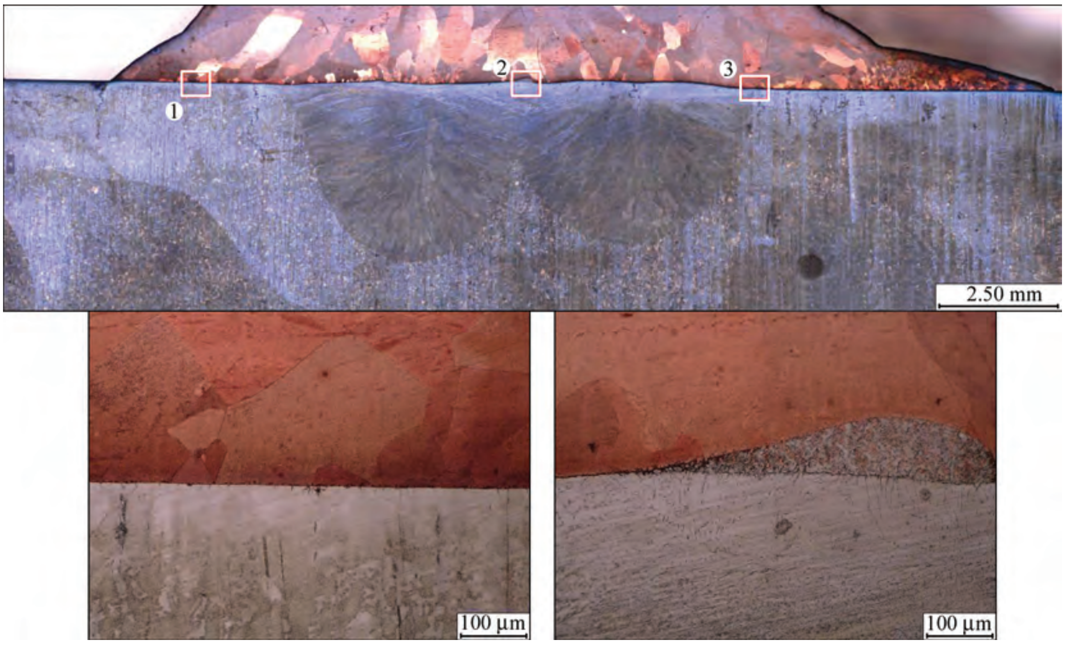

Figure 6. (Upper) Macrograph of etched copper/stainless steel interface demonstrating HAZ in stainless steel as well as variable grain size distribution in the substrate/copper interface. (Bottom-left) Micrograph of copper/substrate interface at region 1 highlighted above, demonstrating sharp boundary between copper and stainless. (Bottom-right) Micrograph of interface region 2, demonstrating copper infiltration into porous stainless steel bump above interface

tion of gas content, density, hardness, electrical conductivity of the 3D printed material, determination of the influence of the process deposition on the residual distortion of conflates, etc.

The electrical conductivity was evaluated using the eddy-current method at 480 kHz, according to ASTM E1004 by comparison with the electrical conductivity value in the traceable reference sample. The

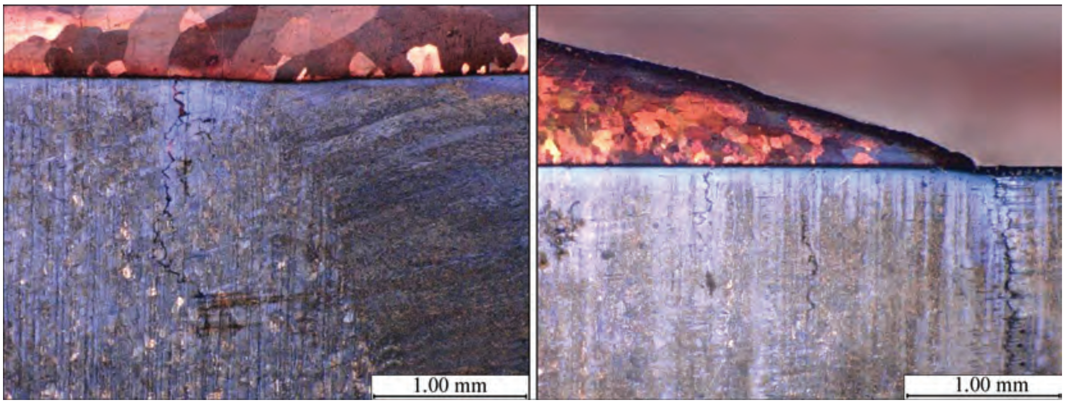

Figure 7. Micrographs of copper/stainless steel interface demonstrating large grain-boundary crack backfilled with copper (left); additional interface cracks at inner edge of deposit (right)

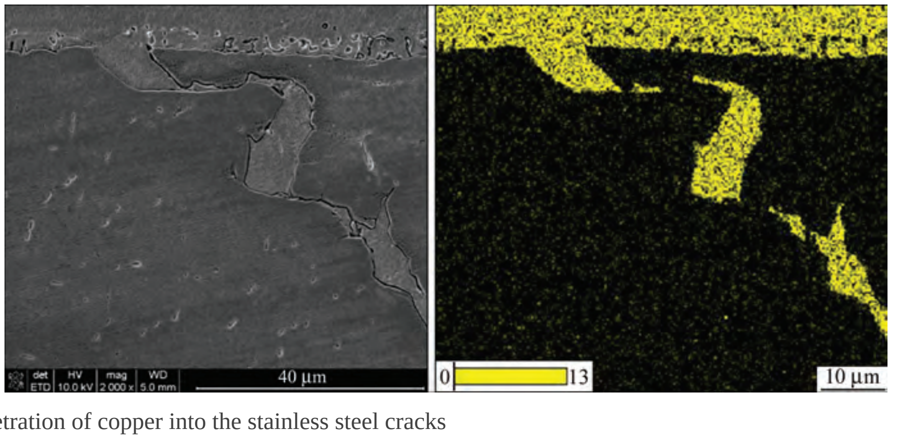

Figure 8. Deep penetration of copper into the stainless steel cracks

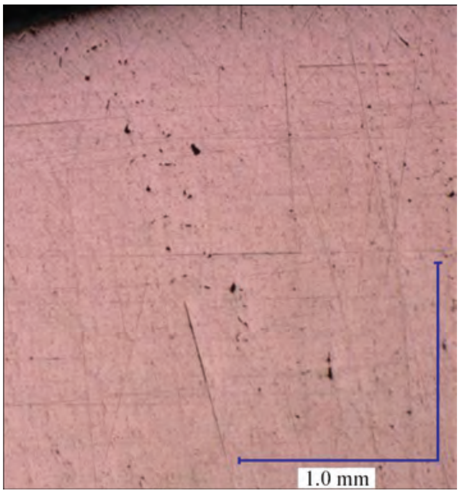

Figure 9. The pore detection area is 1000×1000 μm in size

electrical conductivity 3D printed pure copper was 99.2 (±0.4) % IACS of the reference value.

The oxygen content was measured on LECO equipment according to the requirements of ASTM E1019-18. As a result, the actual oxygen content of the wire used for deposition was 4 ppm, and the oxygen content of three samples cut from different areas of the 3D printed material was 2 ppm — that is, the vacuum 3D printing process provided a certain refinement of pure copper from oxygen, which has positive effect on properties.

Metallographic analysis of the consolidation zone of the two materials showed a dense and strong connection without the formation of new phases. A macrograph of the etched substrate/deposit interface is shown below in Figure 6 with the inner edge of the deposit on the left-hand size. This macrograph demonstrates a heat affected zone (HAZ) in the stainless steel from the first layer deposition, as well as a fine grain copper microstructure at the interface. The fine grain microstructure is especially evident on the

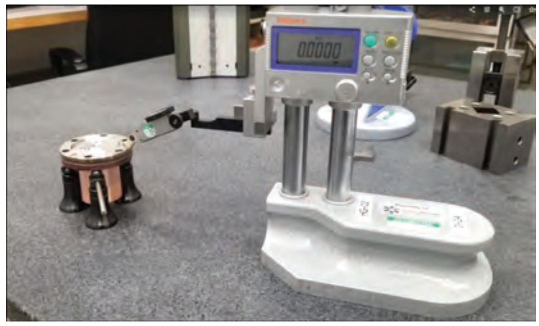

Figure 11. Flatness measurement

leftmost region of the copper deposit, as shown in Figure 7.

A significant number of cracks are observed at the copper/stainless steel interface, which are backfilled with copper, as shown in the micrographs of Figure 7.

Scanning electron microscopy with energy dispersive spectroscopy shows deep penetration of copper into the stainless steel crack (Figure 8).

The density of the 3D printed material was determined by calculating the total area of detected pores in three arbitrarily selected zones measuring 1000×1000 μm each (Keyence grain area analysis) using special software.

In this way, an approximate density of about 99.1 % was determined, which is probably explained by the presence of a large number of small pores ranging in size from units to tens of microns (Figure 9). The variety of shapes and sizes of pores indicate the different nature of their formation — from insufficient fusion of layers to the release of impurity vapors in closed zones during the melting process.

Vickers microhardness was performed at the triple point of the stainless steel fusion zone boundary and the copper deposit, which is region 3 of Figure 6 above. The hardness values show that the stainless steel retains its hardness after deposition of approxi-

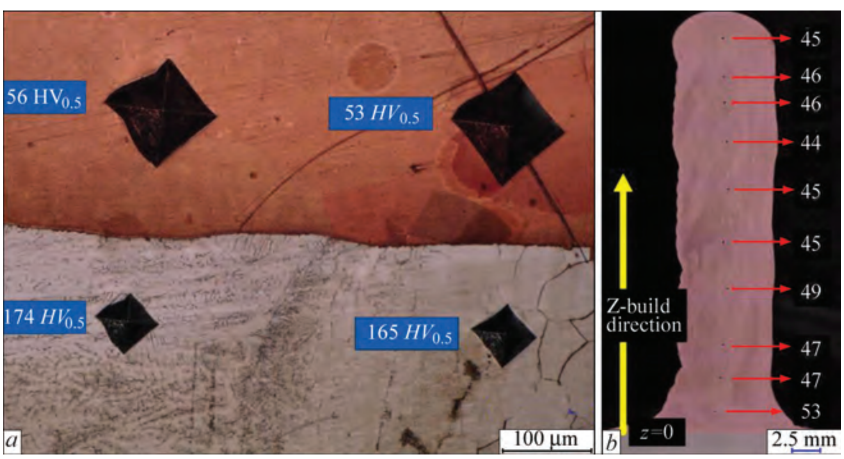

Figure 10. Determination of microhardness and its dependence on height: *a* — microhardness along the length of the deposit following direction of samples growth; *b* — Vickers microhardness at stainless steel fusion zone/base metal/copper interface, at location <3> of Figure 6; *c* — diagram of the dependence of microhardness on the distance from the substrate in the direction of sample growth

Figure 12. Measurement of the helium leakage of the conflate joint (*a*) and the contact surface between the deposited material (copper) and the substrate (stainless steel conflate) (*b*)

mately 165 *HV*, while the copper at the interface has a hardness of annealed, dead-soft copper.

The microhardness of the 3D printed copper was measured along the direction of sample growth (see Figure 10, *a*) as demonstrated in Figure 10, *b*. The obtained data presented in the diagram (Figure 10, *c*) show fairly uniform Vickers microhardness values with some tendency to decrease with distance from the substrate. This is probably related to the number of heating-cooling thermocycles, which decreases with increasing layer number, i.e. with height. Small deviations from the average values indicate the uniformity of the structure of the deposited material.

As already mentioned above, the ability to prevent or minimize residual distortions of the substrate (conflates) under the influence of thermal processes during the consolidation is almost the most important factor in assessing the suitability of the method of obtaining a consolidated joint of copper with a stainless steel conflate.

The flatness (evenness) of the conflate was checked on the side opposite to the 3D printed cylinder. The measurement was made using a calibrated digital indicator with an accuracy of 0.0025 mm (0.0001″) (Figure 11).

In the same way, the flatness of the reference conflat (without the 3D printed copper cylinder) was checked.

The flatness of the reference conflate was <0.0127 mm (0.0005″), and the flatness of the tested sample obtained by 3D printing using xBeam technology was 0.03 mm (0.0012″). That is, it was detected that the residual distortion caused by thermal processes appeared during 3D deposition, but the additional deviation from flatness due to such distortion was very small — no more than 0.0173 mm (0.0007″).

In order to assess how critical the influence of the identified conflate deformation is on the vacuum tightness of the conflate joint, helium leak rate was measured using a high-precision helium detector (Figure 12, *a*). Helium leakage through the contact surface between the deposited material (copper) and the substrate (stainless steel conflate) was also measured (Figure 12, *b*).

In both cases, the absence of any leakage (within the measurement error) was found, which proved the absolute vacuum tightness of both the consolidated copper-stainless steel bimetallic product and the conflate joint using this product. This tests also demonstrated that the deformation of the substrate enabled a hermetic UHV seal on the premachined knife edge.

CONCLUSIONS

Exploratory studies of a consolidated copper-stainless steel bimetallic product formed by 3D printing of a thick-walled cylinder of high-purity copper onto a stainless steel conflate using xBeam 3D metal printing technology demonstrated the following:

- The technological process described above ensured the creation of a strong and absolutely vacuum tight joint of copper with stainless steel, which is confirmed by the absence of helium leakage through the contact surface between the two materials;
- The 3D printing process of formation of a thick-walled copper cylinder upon the substrate of a stainless steel conflate caused only a slight residual deformation of no more than 0.0173 mm (0.0007″), which did not affect the sealing properties of the conflated joint;
- The deposited material (pure copper) has excellent physical properties with no oxygen pickup, sufficient to ensure the functional properties of the consolidated bimetallic product for its intended use;
- xBeam 3D metal printing technology is a promising method of creating consolidated, dissimilar metal joints of materials with different thermophysical and physicochemical properties due to a number of characteristic parameters of the layer-by-layer deposition process, first of all, excellent control of metallurgical processes in and around the melt pool during deposition.

REFERENCES

1. Gaurang R. Joshi et al. (2022) The joining of copper to stainless steel by solid-state welding processes: A Review. *Materials*, 15(**20**), 7234. DOI: https://doi.org/10.3390/ma15207234
2. Raghavendra S. Darji et al. (2021) Exploiting the challenges of copper to austenitic stainless steel bimetallic joining by gas tungsten arc welding: A fluid flow perspective. In: *Proc. of IOP Conf. on Materials Sci. and Eng.*, **1146**, 012011. DOI: https://doi.org/10.1088/1757-899X/1146/1/012011

3. Gu, X., Cui, Z., Gu, X., Shao, J. (2021) Wire-feeding laser-welding of copper/stainless steel using different filler metals. *Materials*, 14(**9**), 2122. DOI: https://doi.org/10.3390/ma14092122
4. Turna, M., Sahul, M., Ondruska, J., Lokaj, J. (2011) Electron beam welding of copper to stainless steel. In: *Proc. of Inter. DAAAM Symp., Vienna, Austria*. Ed. by B. Katalinic. Vol. 22, 833–834.
5. Sahul, M., Sahul, M., Turˇna, M., Zacková, P. (2014) Disk laser welding of copper to stainless steel. *Adv. Mater. Res.*, **1077**, 76–81. DOI: https://doi.org/10.4028/www.scientific.net/AMR.1077.76
6. Osipovich, Kseniya S. et al. (2020) Gradient transition zone structure in "steel–copper" sample produced by double wire-feed electron beam additive manufacturing. *J. of Materials Sci.*, **55**, 9258-9272. DOI: https://doi.org/10.1007/s10853-020-04549-y
7. Rock, Christopher et al. (2021) Characterization of copper & stainless steel interface produced by electron beam powder bed fusion. *Materials & Design*, **212**, 110278. DOI: https://doi.org/10.1016/j.matdes.2021.110278
8. Kovalchuk, D.V., Melnik, V.I., Melnik, I.V., Tugaj, B.A. (2017) New possibilities of additive manufacturing using xBeam 3D Metal Printing technology (Review). *The Paton Welding J.*, **12**, 16–22. DOI: https://doi.org/10.15407/tpwj2017.12.03
9. Kovalchuk, D., Ivasishin, O. (2019) Profile electron beam 3D metal printing. In: *Additive Manufacturing for the Aerospace Industry*, 213–233. DOI: https://doi.org/10.1016/B978-0-12-814062-8.00012-1
10. Makhnenko, O.V., Milenin, A.S., Velikoivanenko, E.A. et al. (2017) Modelling of temperature fields and stress-strain state of small 3D sample in its layer-by-layer forming. *The Paton Welding J.*, **3**, 7–14. DOI: https://doi.org/10.15407/tpwj2017.03.02

ORCID

D. Kovalchuk: 0000-0001-9016-097X,
P.R. Carriere: 0000-0002-4793-5239,
Nanda Gopal Matavalam: 0009-0005-0676-6394

CONFLICT OF INTEREST

The Authors declare no conflict of interest

CORRESPONDING AUTHOR

D. Kovalchuk
JSC NVO Chervona Hvilya
28 Dubrovytska Str., 04200, Kyiv, Ukraine.
E-mail: dmytro@xbeam3d.com

SUGGESTED CITATION

D. Kovalchuk, L. Tretiakov, P.R. Carriere, Nanda Gopal Matavalam (2024) Manufacturing a consolidated copper-stainless steel bimetallic product using xBeam 3D metal printing. *The Paton Welding J.*, **7**, 3–9.
DOI: https://doi.org/10.37434/tpwj2024.07.01

JOURNAL HOME PAGE

https://patonpublishinghouse.com/eng/journals/tpwj

Received: 31.01.2024
Received in revised form: 12.04.2024
Accepted: 29.07.2024